

# **An Algorithmic 3D Rock Roughness Measure Using Local Depth Measurement Clusters**

By

**H. H. W. Herda**

Department of Mathematics, University of Massachusetts, Boston, MA, U.S.A.

Received March 31, 2004; accepted April 27, 2005  
Published online July 19, 2005 © Springer-Verlag 2005

## **Summary**

A computational algorithm which uses depth data from a reference plane to a rock fracture surface in calculating a new three-dimensional joint roughness coefficient is presented. Two independent sets of fracture data are investigated. The new coefficient is compared to Barton's 2D joint roughness coefficient JRC. A measure indicating corrupt data is discussed. The algorithm is also used to show that, in general, rock roughness is only a local variable, not a directional one.

*Keywords:* Rock roughness, algorithm, joint roughness coefficient.

## **1. Introduction**

Barton's joint roughness coefficient, JRC, (see Barton and Choubey, 1977, p. 7) has gained universal acceptance in rock mechanics. However, its current application often has two major difficulties. The first is that the fracture (joint) surface is three-dimensional but the JRC is estimated from two-dimensional profiles chosen from the surface. The second is that this estimation is often done visually using a group of ten typical roughness profiles (see Barton and Choubey, 1977, p. 19). We develop an algorithm which relies on local clusters of depth data and is implemented on a computer. The algorithm has been experimentally calibrated so that the final number which it yields agrees well with Barton's JRC for a range of sample specimens. This number is the new, algorithmic JRC, here denoted as JRC3. It is ready for use at least in the 0.25 mm to 1 mm sampling range. The algorithm is designed for depth data measured from a reference plane square grid roughly normal to the joint surface.

## **2. Description of First Specimen Set and of Data Gathering**

These specimens (see Fig. 1a) are 8 cm × 12 cm cast concrete blocks of rock fractures labeled OBL, NBL, LBU, MBU, and KBL, in increasing degree of roughness. The

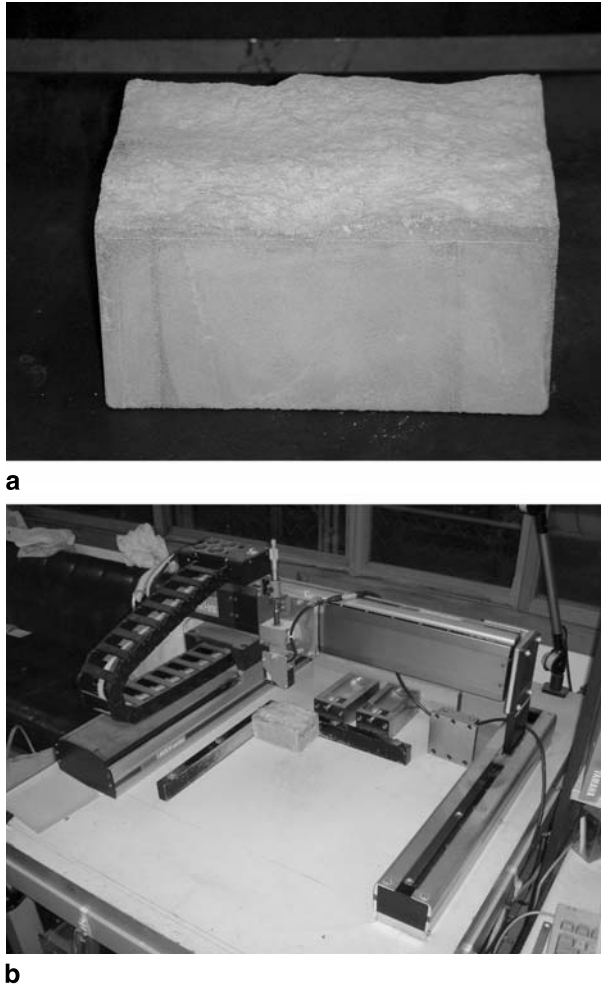


**Fig. 1. a** Sample specimen block; **b** measuring apparatus

depth data were measured using a laser instrument (see Fig. 1b) at 0.25 mm intervals on vertical tracks also 0.25 mm apart. Thus, there is a 0.25 mm scale of measurement. Professor Ohnishi (2004) of Kyoto University provided the author with these data. For the first three blocks the measurements are complete and can be represented as a 317 row  $\times$  477 column matrix or as a vector of length 151209. We chose the vector form for the algorithm and formed the vector  $a$  (with  $a(151209)$  as its last element).

MBU is missing eight measurements and KBL is missing 18 measurements. These measurements are always missing at the end of one or more of the 477 columns and we succeeded in padding the ends of the relevant columns with locally average inserts. For example (see Fig. 2), if all prior columns of depth data are complete and the 66<sup>th</sup> column's first 314 entries nearly match those in the same row of the 65<sup>th</sup> column but

	Col. 65	Col. 66	Col. 67
Row 1	36.4	36.3	36.6
Row 2	36.3	36.5	36.4
Row 3	36.3	36.4	36.5
Row 4	36.4	36.5	36.3
.	.	.	.
.	.	.	.
.	.	.	.
Row 312	40.8	40.7	40.7
Row 313	40.7	40.8	40.9
Row 314	40.8	40.9	40.8
Row 315	40.8	<i>40.9</i> → 36.5	36.6
Row 316	40.9	<i>40.9</i> → 36.4	36.6
Row 317	41.0	<i>40.9</i> → 36.3	36.5

Fig. 2. Simplified 0.25 mm depth data. End-of-column padding in col. 66. Inserts in italic type

the last 3 entries do not (instead they will nearly match the first three entries of column 67 because they belong at the top of column 67), we pad the end of column 66 by inserting 3 ad-hoc entries (here each is 40.9) which are close in value to the last three entries in column 65. This bumps the formerly mismatched 3 entries up to the top of column 67 since we are really computing in a vector array. Note that column 67 and all further columns will also be corrected. This padding may have to be done several times in some succeeding columns.

### 3. Computations Leading to the Algorithmic JRC3

All computations are done on a Dell PC in MatLab. The basic 54-line script is shown for reference in the Appendix (Section 9). We decided on a local determination of roughness using  $5 \times 5$  clusters of measurements because rock roughness at or near the millimeter scale is a strictly locally varying phenomenon. This will be established at the end of the paper, in Section 7. We use the same notation for a measurement value and for the location at which it is taken.

The first center of such a  $5 \times 5$  (square) group is at a(637) (see Fig. 3). When looking at Fig. 3, think of the specimen block as situated below and your view as roughly perpendicular to the fracture surface. We now compute a partial sum in the first square cluster of measurements, shown in Fig. 3, as follows: the center is at a(637). The square of the absolute value of the difference between a(637) and each of its twenty-four first- and second-neighbors is determined. a(320), a(636), a(638), and a(956) have squared distance 1 unit (=0.25 mm) from center a(637); a(319), a(321), a(955), and a(957) have squared distance 2 units from a(637); a(3), a(635), a(639), and a(1273) have squared distance 4 units; a(2), a(4), a(318), a(322), a(954), a(958), a(1272), and a(1274) all have squared distance 5; a(1), a(5), a(1271), and a(1275) have squared distance 8. To properly weigh their contributions, the various squared absolute differences of the depths are divided by the corresponding squared

(top edge of block)

(left edge of block)	a(1)	a(318)	a(635)	a(954)	a(1271)	...
	a(2)	a(319)	a(636)	a(955)	a(1272)	...
	a(3)	a(320)	a(637)	a(956)	a(1273)	...
	a(4)	a(321)	a(638)	a(957)	a(1274)	...
	a(5)	a(322)	a(639)	a(958)	a(1275)	...
	...	...	...	...	...	...

Fig. 3. The first square group of measurements

distances from a(637). These twenty-four non-negative numbers are added to form location a(637)'s non-negative partial sum which is stored as the first element in a new b-vector.

This process is repeated with the next  $5 \times 5$  square group centered at a(638), resulting in the next element of the b-vector, and then continued (with a total of 313 centers in this column) until the center at a(949). It is then continued with 313 centers in the next column, from a(954) to a(1266), and so on. Altogether, the process involves 473 columns of centers and ends at center a(150573), as seen in Fig. 4. It is important to compute these partial sums of overlapping groups in order not to miss any large first- or second-neighbor squared absolute differences.

There are  $313 \times 473 = 148049$  centers, partial sums, and elements in the b-vector. For example, let the b-vector be [1.4, 0.3, 1.9, 1.1, 5.3]. The elements of the b-vector are now counted (by binning) into a new c-vector so that  $c(i)$  is the number of b-vector elements less than  $i$ , for  $i = 1, 2, 3, \dots, mx$ , where  $mx$  is the number of bins (the bin count), equal to the least integer larger than the maximum

...	...	...	...	...	(right edge of block)
a(149937)	a(150254)	a(150571)	a(150888)	a(151205)	
a(149938)	a(150255)	a(150572)	a(150889)	a(151206)	
a(149939)	a(150256)	a(150573)	a(150890)	a(151207)	
a(149940)	a(150257)	a(150574)	a(150891)	a(151208)	
a(149941)	a(150258)	a(150575)	a(150892)	a(151209)	

(bottom edge of block)

Fig. 4. The last square group of measurements

b-vector element. In our example the bin count is  $m_x = 6$  and the c-vector becomes [1, 4, 4, 4, 4, 5].

The bin count gives an indication of spalling at the block edges and of corrupt data due to incorrect or missing padding. In both cases, very large b-vector elements are due to (spurious) large differences in adjacent depth measurements. Both conditions can result in bin counts in the 200 to 1000 range at the 0.25 mm scale. Corrupt data may lead to bin counts exceeding 6000. Spalling can be corrected for by removing a border of two rows and two columns of measurements all around the edges. This causes a less than 0.5% change in JRC3. Incorrect padding can give very large errors. There are specimens for which successful padding appears impossible. For our specimens the bin count  $m_x$  ranges from 97 to 167 at the 0.25 mm scale; at larger scales, the bin count never exceeds 60.

The power-weighted sum

$$w = \sum_{m=1}^{(m_x-1)} m^{0.537} |c(m+1) - c(m)|$$

is now computed. For an example of the w-computation let the b-vector be [1.4, 0.3, 1.9, 1.1, 5.3] as in our last example. Then the bin count  $m_x = 6$  and the c-vector is [1, 4, 4, 4, 4, 5]. The weighted sum is  $w = 1^{0.537}|4 - 1| + 2^{0.537}|4 - 4| + 3^{0.537}|4 - 4| + 4^{0.537}|4 - 4| + 5^{0.537}|5 - 4| \approx 5.37$ . The actual value of w typically ranges from around 180000 to about 320000.

The factor  $|c(m+1) - c(m)|$  measures the overall rate at which roughness is increasing for each value of m. We multiplied this factor with  $m^{\text{power}}$  as a consequence of mathematical experiments. We chose the power 0.537 because it maximizes the correlation between Ohnishi's JRC and w at the 0.25 mm measurement scale as  $r \approx 0.9962$ . This correlation is quite stable, with  $r > 0.9944$  for powers in the range 0.325 to 0.790. We chose the 0.25 mm scale because its measurements give the greatest amount of information about these rock fractures. The weighted sum w captures the aggregate of these effects over the whole rock joint surface.

The so-called "rough" is calculated as  $w/30000$  in order to yield a value less than twenty or so, for use in Table 1 and Tables 3–5. This linear change of scale will not change the coefficient r in correlations yet to be described. Execution of the script takes about ten seconds for the specimens without padding, but about four minutes for MBU, which needed padding near the beginning of its measurement vector. The insertions and vector manipulations required are time-consuming in MatLab.

**Table 1.** Comparison of JRC/JRC3 values at 0.25 mm scale

	OBL	NBL	LBU	MBU	KBL
Rough	5.8388	6.0113	7.0645	7.7757	9.8652
JRC (Ohnishi)	5.5	7.4	10.7	12.7	20.0
JRC3	6.20	6.79	10.41	12.86	20.04
Bin count	97	131	113	157	167

$r \approx 0.9962$ , Least squares line:  $m \approx 3.4368$ ,  $b \approx -13.8673$ .

**4. Calibration of JRC3 with Barton’s JRC**

Professor Ohnishi (2004) provided the author with the Barton JRC of the specimen blocks mentioned earlier (see Section 2). These 2D JRC values were determined using Tse and Cruden (1979) as well as Yu and Vayssade (1991). The correlation coefficient between our “rough”  $w/30000$ -values obtained by executing the Matlab script in Section 9 as necessary (minus the last two lines and instead displaying  $w/30000$  at the end) and the corresponding Ohnishi JRC values is computed with a calculator, as are the slope and intercept of the least-squares line. The correlation coefficient is  $r \approx 0.9962$ . This slope and intercept are used to calculate JRC3 values from the “rough” values (see Table 1). The correlation coefficient between JRC and JRC3 is again unchanged under the linear transformation.

**5. Investigation of JRC3 at Larger Scales**

We begin by using the same five specimen blocks but first changing to a measurement scale of 0.5 mm and picking up only about one-fourth as many measurements. To retain the approximate size of the rough numbers, we reduce the divisor of  $w$  proportional to the number of centers (see Table 2). This is optional because the size of the constant divisor does not affect the correlation coefficient or the value of JRC3 at a given scale. The results for 0.5 mm are summarized in Table 3. The correlation coefficient  $r \approx 0.9926$  is lower than for the 0.25 mm scale, partly because only one-fourth of the data are available, and they are employed differently by the algorithm.

Again using the five specimen blocks, we change to a 1 mm measurement scale while gathering only about one-fourth as many measurements as in the last round. These results are summarized in Table 4. The correlation coefficient  $r \approx 0.9799$  is again lower but the fit between JRC and JRC3 is still good.

**Table 2.** Algorithm divisors at various scales

Scale	No. of centers	Divisor
0.25 mm	144921	30000
0.5 mm	35649	7380
... B ... 1 mm	8436	1746
KY_... 1 mm	11988	2482

**Table 3.** Comparison of JRC/JRC3 values at 0.5 mm scale

	OBL	NBL	LBU	MBU	KBL
Rough	5.2410	5.3642	5.8345	6.3374	7.6924
JRC (Ohnishi)	5.5	7.4	10.7	12.7	20.0
JRC3	6.46	7.15	9.80	12.63	20.26
Bin count	44	44	44	60	45

$r \approx 0.9926$ , Least squares line:  $m \approx 5.6311$ ,  $b \approx -23.0556$ .

**Table 4.** Comparison of JRC (Ohnishi)/JRC3 at 1 mm scale

	OBL	NBL	LBU	MBU	KBL
Rough	5.0647	5.1819	5.3831	5.9328	7.0167
JRC (Ohnishi)	5.5	7.4	10.7	12.7	20.0
JRC3	6.85	7.62	8.95	12.57	20.32
Bin count	44	44	44	44	45

$r \cong 0.9799$ , Least squares line:  $m \cong 6.5958$ ,  $b \cong -26.5592$ .

**6. Description of Second Specimen Set**

Now we introduce three 12 cm × 12 cm cast concrete blocks of rock joints KY\_A, KY\_C, and KY\_E. For these, depth measurements were made by hand (over ten years ago) at the 1 mm scale, using a specially constructed steel rig. The measurements were transferred to floppy discs provided to the author by Professor Ohnishi (1993) and eventually re-formatted for use with MatLab scripts. We had no Barton JRC values available for these blocks. We therefore estimated the roughness of the very rough fracture KY\_E and show four typical profiles (see Figs. 5– 8). The JRC range numbers shown in the figures are averaged and produce JRC 18.5. For KY\_A, not quite as rough, we show two typical profiles in Figs. 9, 10. We estimate KY\_A to have roughness JRC 18. KY\_C is rather smooth, as seen in two profiles shown in Figs. 11, 12. It is estimated to have roughness JRC 6. (An interesting, albeit somewhat unrelated, observation is that at or near the millimeter scale these 2D profiles and 2D profiles of the author’s five 3D specimens mentioned earlier (see Section 2) do not show self-similar or fractal behavior, which has been documented in 2D, e.g. by Murata and Saito (2003), and by Odling (1994).)

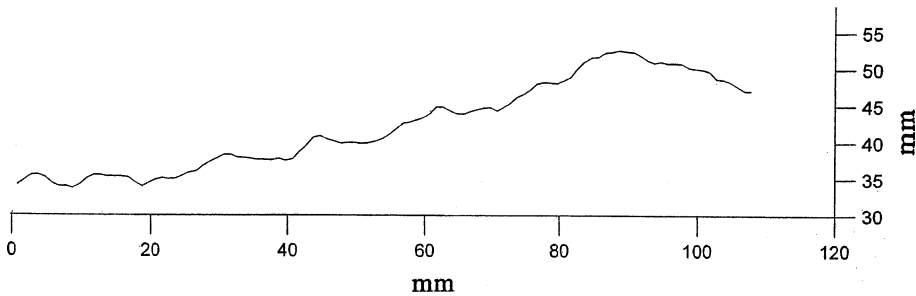


**Fig. 5.** KY\_E, row 89: JRC 18–20

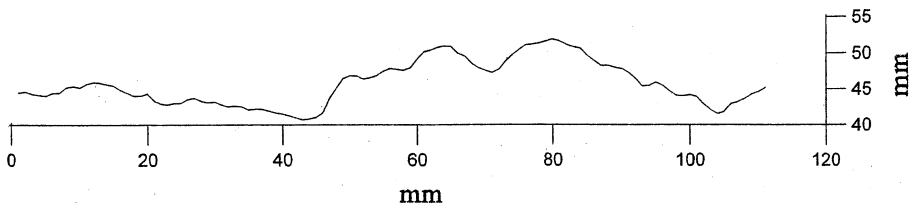


**Fig. 6.** KY\_E, column 91: JRC 18–20

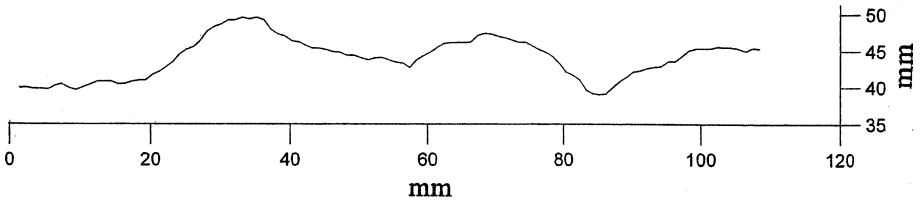


Fig. 7. KY\_E, row 26: JRC 18-20

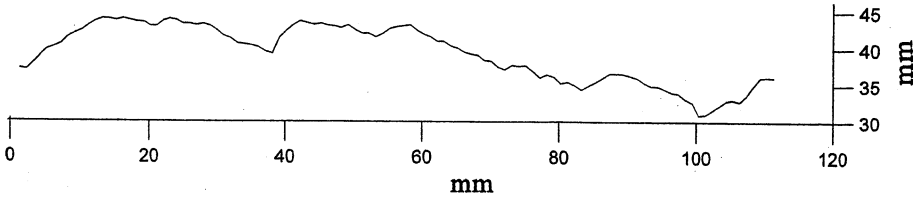


Fig. 8. KY\_E, column 18: JRC 16-18

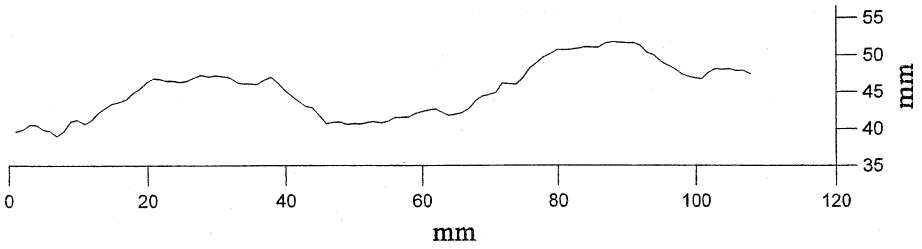


Fig. 9. KY\_A, row 16: JRC 18-20

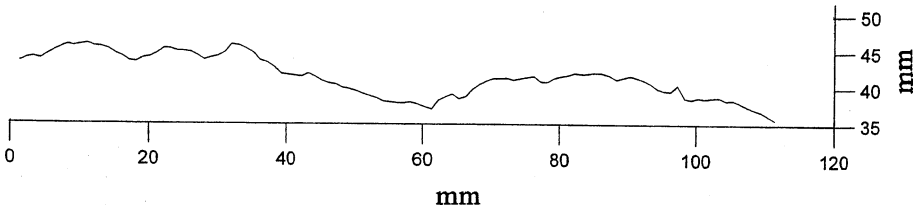


Fig. 10. KY\_A, column 109: JRC 16-18

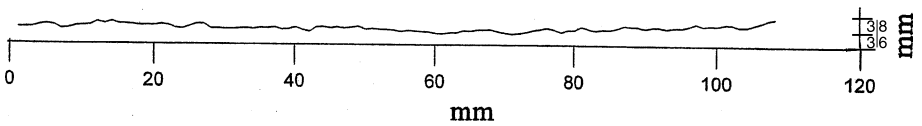


Fig. 11. KY\_C, row 62: JRC 6-8

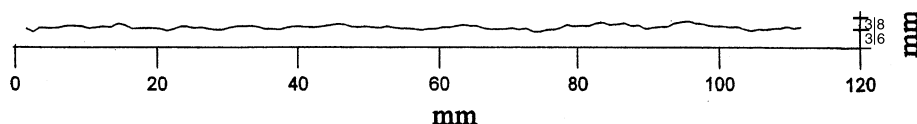


Fig. 12. KY\_C, column 109: JRC 4–6

Table 5. Comparison of JRC (Author)/JRC3 values at 1 mm scale

	KY_A	KY_C	KY_E
Rough	11.2051	5.1183	11.7109
JRC (Author)	18.0	6.0	18.5
JRC3	17.75	6.02	18.73
Bin count	35	6	34

$r \cong 0.9994$ , Least squares line:  $m \cong 1.9278$ ,  $b \cong -3.8480$ .

Table 6. Comparison of all JRC/JRC3 values at 1 mm scale

	OBL	NBL	LBU	MBU	KBL	KY_A	KY_C	KY_E
JRC	5.5	7.4	10.7	12.7	20.0	18.0	6.0	18.5
JRC3	6.85	7.62	8.95	12.57	20.32	17.75	6.02	18.73

$r \cong 0.9898$ .

When the algorithm is applied to these specimens, it produces JRC3 values extremely close to the estimated JRC values (see Table 5). The correlation coefficient  $r$  is  $\approx 0.9994$ , but there are only three data points. A better test is to combine the eight 1 mm scale JRC/JRC3 roughness results, shown in Table 6. Here the correlation coefficient is  $r \approx 0.9898$ . This suggests that JRC3 does not depend on the measuring equipment because some specimens in Table 6 were depth-measured using a laser while the others were depth-measured by hand. These results together suggest that JRC3 provides reliable estimates of rock roughness at the 0.25 mm scale as well as at 0.5 mm and 1 mm scales using the 0.537 power in the algorithm. The algorithm is ready for use on rock measured at these scales or at an intermediate scale, possibly also at a somewhat smaller scale.

### 7. Evidence of Purely Local Variability of Rock Roughness

It has been thought that rock fracture roughness in three dimensions is a property essentially constant in a given direction, but this is not the case. We sampled the rough 8 cm × 12 cm KBL block at the 0.25 mm scale using rectangular strips of measurement, each 12 cm long and normal to the block’s short edge, and each covering about 8% of the area of the whole block (see Fig. 13). The variation in roughness of these strips, as they are moved by 0.25 mm parallel steps from the top of the block to the bottom, is shown in Fig. 14. The figure also shows that the joint roughness coefficient is an average value calculated over the whole rock surface.

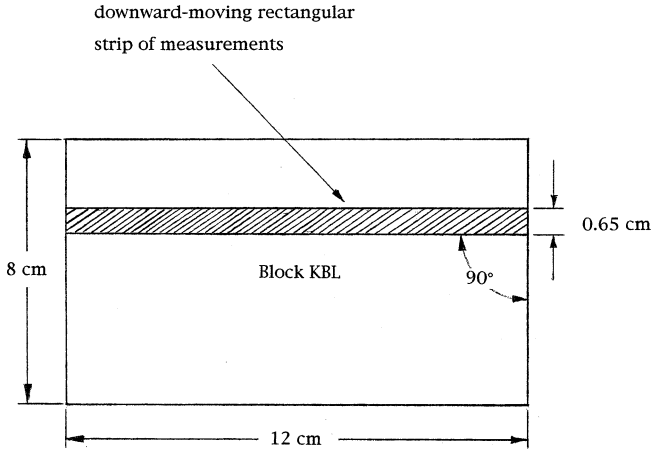


Fig. 13. Motion of measurement strip on block KBL

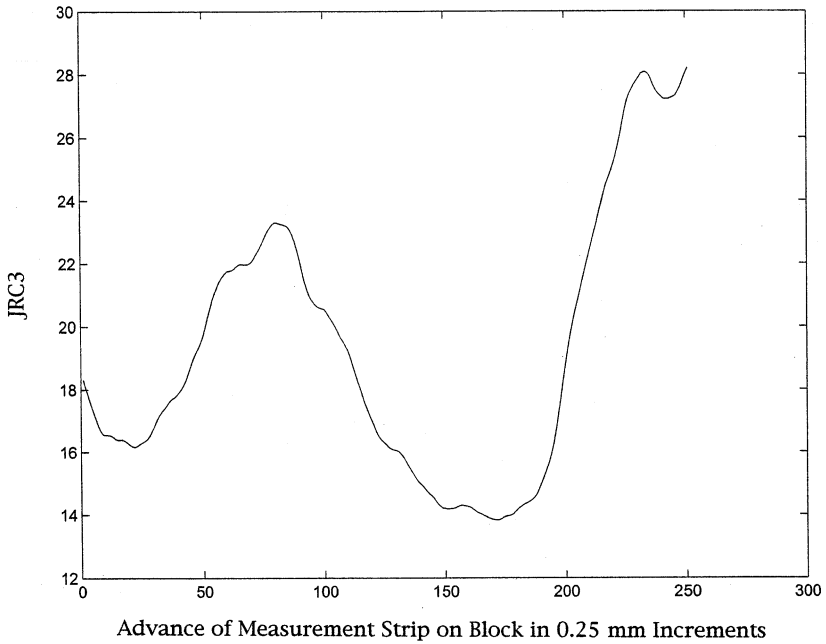


Fig. 14. Roughness variability on sections of block KBL

### 8. Conclusion

An algorithm yielding the three-dimensional rock roughness coefficient JRC3 suitable for depth data gathered at a scale between 0.25 mm and 1 mm from a reference plane subparallel to a joint surface is described. Its use is investigated on two sets of fracture

data. Comparison of JRC3 to Barton's JRC yields correlations between 0.9799 and 0.9994. A bin count measure indicating corrupt data is discussed. The algorithm is also employed to show that rock roughness generally varies only locally and is not constant along a given direction.

## 9. Appendix: MatLab Script Implementing the Algorithm

```
[a]=textread('OBL02vector.txt','%f'); % Block OBL Roughness at 0.25mm Scale
for k=3:471 % column index of center (both side borders decreased by 0.5mm)
  for h=3:311 % row index of center (top & bottom borders decreased by 0.5mm)
    i=317*k+h+319; % location of centers; there are 148049 centers
    ai=a(i); % center
    l=(ai-a(i-317))^2; % left 0.25mm = 1 unit; meas. of squared diff. with a(i)
    r=(ai-a(i+317))^2; % right 1
    u=(ai-a(i-1))^2; % up 1
    d=(ai-a(i+1))^2; % down 1
    lu=(ai-a(i-318))^2/2; % left 1 & up 1 (all the rest are divided by the
    ru=(ai-a(i+316))^2/2; % right 1 & up 1 square of the unit distance between
    ld=(ai-a(i-316))^2/2; % left 1 & down 1 lattice points)
    rd=(ai-a(i+318))^2/2; % right 1 & down 1
    first=l+r+u+d+lu+ru+ld+rd; % 1st-neighbor sum of weighted squares of diffs.
    l2u2=(ai-a(i-636))^2/8; % left 2 & up 2
    l2u1=(ai-a(i-635))^2/5; % left 2 & up 1
    l2=(ai-a(i-634))^2/4; % left 2
    l2d1=(ai-a(i-633))^2/5; % left 2 & down 1
    l2d2=(ai-a(i-632))^2/8; % left 2 & down 2
    l1u2=(ai-a(i-319))^2/5; % left 1 & up 2
    l1d2=(ai-a(i-315))^2/5; % left 1 & down 2
    u2=(ai-a(i-2))^2/4; % up 2
    d2=(ai-a(i+2))^2/4; % down 2
    r1u2=(ai-a(i+315))^2/5; % right 1 & up 2
    r1d2=(ai-a(i+319))^2/5; % right 1 & down 2
    r2u2=(ai-a(i+632))^2/8; % right 2 & up 2
    r2u1=(ai-a(i+633))^2/5; % right 2 & up 1
    r2=(ai-a(i+634))^2/4; % right 2
    r2d1=(ai-a(i+635))^2/5; % right 2 & down 1
    r2d2=(ai-a(i+636))^2/8; % right 2 & down 2; nxt. line: 2nd nbr. wgh. sq. diffs. sum
    second=l2u2+l2u1+l2+l2d1+l2d2+l1u2+l1d2+u2+d2+r1u2+r1d2+r2u2+r2u1+r2+r2d1+r2d2;
    b(i)=16*(first+second); % sum of all 1st- and 2nd-nbr. weighted sq. diffs. at a(i)
    % are stored in vector b
  end
  % 16 is scaling factor for 0.25mm scale
  % (4 is scaling factor for 0.5mm scale)
end
mx=floor(max(b))+1; % no. of bins
for g=1:mx % binning of b-values
  z=0;
  for k=3:471
    for h=3:311
      j=317*k+h+319;
      if b(j)>=(g-1)
        z=z+1; % counts no. of weighted sq. difference sums >=(g-1)
      end
    end
  end
  c(g)=z; % no. of values of b(i)>=(g-1) are stored in vector c
end
w=0;
n=mx-1;
for m=1:n
  w=w+m^0.537*abs(c(m)-c(m+1)); % scaling of weighted sum
end
jrc3=w*3.4369/30000-13.8674 % computation of jrc3 from rough = w / 30000
display(mx) % allows check on corrupt data and spalling
```

### Acknowledgements

The author thanks Professor Yuzo Ohnishi of the Department of Urban and Environmental Engineering in the Graduate School of Engineering of Kyoto University, who provided him with the depth data on KY\_A, KY\_C, and KY\_E while the author was his guest during a sabbatical year. He recently provided the author with depth data on OBL, NBL, LBU, MBU, and KBL. The author also thanks Dr. Patrick Bruines of the same Department for Fig. 1a and b. Thanks are due as well to the author's former student Arvald Karp for re-formatting the KY\_A, KY\_C, and KY\_E depth data.

### References

- Barton, N., Choubey, V. (1977): The shear strength of rock joints in theory and practice. *Rock Mech.* 10, 1–54.
- Murata, S., Saito, T. (2003): A new evaluation method of JRC and its size effect. 10<sup>th</sup> Intl. Conf. Intl. Soc. Rock Mech. Vouille & P. Berest, Paris, 855–858.
- Odling, N. E. (1994): Natural fracture profiles, fractal dimension and joint roughness coefficients. *Rock Mech. Rock Engng.* 27(3), 135–153.
- Ohnishi, Y. (1993): Personal communication of laboratory data.
- Ohnishi, Y. (2004): Personal communication of laboratory data.
- Tse, R., Cruden, D. M. (1979): Estimating joint roughness coefficients. *Int. J. Rock Mech. Min. Sci.* 16, 303–307.
- Yu, X., Vayssade, D. (1991): Joint profiles and their roughness parameters. *Int. J. Rock Mech. Min. Sci.* 28(4), 333–336.

**Author's address:** Prof. Hans Herda, M.I.T., 77 Massachusetts Avenue, Room 1-330, Cambridge, MA 02139, U.S.A.; e-mail: hans@math.umb.edu